Electroacupuncture regulates inflammation, collagen deposition and macrophage function in skeletal muscle through the TGF-β1/Smad3/p38/ERK1/2 pathway

HONG HAN[1*], MING LI[2*], HUILIN LIU[3] and HAOHAN LI[4]

[1]Department of Rehabilitation Medicine, Wuhan Fourth Hospital, Wuhan, Hubei 430000; [2]Department of Rehabilitation, Hubei Provincial Hospital, Wuhan, Hubei 430071; [3]Department of Neurological Physical Therapy, China Rehabilitation Research Center, Bo Ai Hospital, Beijing 100068, P.R. China; [4]The Facility of Business and Law, Deakin University Health Faculty, Geelong, Victoria 3220, Australia

Received March 1, 2021; Accepted September 1, 2021

DOI: 10.3892/etm.2021.10892

Abstract. Skeletal muscle injury is one of the most common sports injury, which accounts for ~40% of all sports-related injuries among the elderly. In addition, cases of full recovery from treatment are rare. Although electroacupuncture (EA) is an integral aspect of traditional Chinese medicine, the effects of EA on skeletal muscle fibrosis and the possible underlying mechanism remain unclear. To investigate the effect and potential mechanism of EA on skeletal inflammation, collagen deposition and macrophage function, a skeletal muscle injury model was established by injecting 100 μl cardiotoxin into the anterior tibial muscle of Sprague Dawley rats. The animals were randomly divided into the following three groups: Control, model and EA. The expression of inflammation-related factors (IL-6, IL-4, IL-33, IL-10 and TNF-α) were measured using ELISA. H&E staining, Masson's staining and immunohistochemistry (collagen II, Axin2 and β-catenin) were performed to assess collagen deposition and fibrosis in the muscle tissues. Additionally, immunofluorescence was performed to measure the ratio of M_1 to M_2 macrophages. Western blotting was performed to examine the activity of the TGF-β1/Smad3/p38/ERK1/2 pathway. Compared with that in the control rats, the mental state, such as the degree of activity and excitement, of the model rats deteriorated, with clear activity limitations. Compared with those in the model rats, EA-treated rats exhibited improved mental status and activity, reduced levels of IL-6, IL-4 and TNF-α, reduced collagen deposition and fibrosis, in addition to increased expression of IL-33 and IL-10. This improvement became increasingly evident with prolonged intervention time. EA also promoted the transformation of macrophages from the M_1 into the M_2 sub-type, where the M_1/M_2 ratio on day 7 was lower compared with that on day 14. Western blotting results showed that compared with that in the model rats, the expression of TGF-β1, MMP-2, MMP-7 and the activation of Smad3 and p38 was decreased in EA-treated rats, whilst the activation of ERK1/2 was significantly elevated. In conclusion, EA can inhibit inflammation and collagen deposition whilst promoting the transformation of macrophages from the M_1 into the M_2 sub-type. The underlying mechanism was found to be associated with TGF-β1/Smad3/p38/ERK1/2 signaling.

Correspondence to: Dr Hong Han, Department of Rehabilitation Medicine, Wuhan Fourth Hospital, 473 Hanzheng Street, Wuhan, Hubei 430000, P.R. China
E-mail: han20190807@163.com

[*]Contributed equally

Key words: electroacupuncture, inflammation, collagen deposition, macrophage, TGF-β1.

Introduction

Skeletal muscle injury is one of the most common type of injury in sports, which accounts for ~40% of all sports-related injuries among the elderly (1). Currently available therapeutic strategies to promote skeletal muscle healing after an injury remain unsatisfactory, which is mainly due to skeletal muscle fibrosis, which frequently hinders full functional recovery (2-4). In addition, skeletal muscle fibrosis results in limited movement, resulting in dysfunction and severely affects the quality of life (5). Therefore, it is of clinical importance to study the mechanism underlying fibrosis after skeletal muscle injury and to explore novel treatment methods.

Skeletal muscle injury repair is regulated by the balance between muscle fiber regeneration and fibrosis, where recovery depends on the development of completely regenerated muscle fibers, extracellular matrix and fibrosis (6). The process of injured skeletal muscle repair can be divided into the following three stages: Inflammatory response; repair; and shaping (7). TGF-β1 is a key factor in the development of kidney, liver, lung and skeletal muscle fibrosis (8). In skeletal muscles, TGF-β1 can inhibit myogenic differentiation and activate MAPK signaling, which eventually lead to skeletal muscle fibrosis at the injury site (9,10). Inflammation and immune cells also serve key roles in the regeneration of the skeletal muscle (11,12). TGF-β1 inhibits the conversion of M_1 macrophages into the M_2 type, where growth factors produced by M_1 macrophages, including TGF-β1, platelet-derived growth factor, fibroblast growth factor-2 and VEGF, can subsequently lead to extracellular matrix production (13). Previous studies have shown that the exogenous treatment of M_1 macrophages significantly reduced muscle fibrosis whilst enhancing muscle fiber regeneration (14,15).

Acupuncture is an integral aspect of traditional Chinese medicine and is frequently applied to treat rheumatoid arthritis, acute gastritis and other immune-related diseases (16). It can improve immunity, alleviate inflammation, mediate $CD4^+$ T cell differentiation and dendritic cell maturation, reduce fibrous tissue proliferation and inhibit fibrosis (17). Electroacupuncture (EA, weak electrical stimulation using acupuncture needles) is a type of acupuncture that (18), when combined with exercise therapy, has been demonstrated to exert therapeutic effects on lower back pain due to acute lumbar sprain (19). However, the effects of EA on skeletal muscle fibrosis and the possible underlying mechanism remain unclear. Therefore, in the present study, the potential effects of EA on inflammatory cell infiltration, injury and fibrosis in a model of skeletal muscle injury were evaluated. In addition, the possible mechanism underlying the effects of EA on skeletal muscle fibrosis was also investigated. It is hoped that data from the present study can provide a theoretical basis for the use of EA in treating skeletal muscle fibrosis following injury.

Materials and methods

Animals. A total of 20 Sprague-Dawley rats (sex, nine male and nine female; age, 12 weeks; weight, 250±20 g) were obtained from the Hubei Experimental Animal Research Center (license no. 42000600032492). The animals were housed in a specific-pathogen-free environment in opaque polypropylene cages in a standard 12-h light/dark cycle, at 23±3˚C and 50-60% humidity. Food and water were available *ad libitum*. The rats were allowed to adapt to the aforementioned conditions for 7 days before experimentation.

Following the method previously described by Zhang et al (20), 100 µl cardiotoxin (CTX; 10 µM; 0.028 mg/kg) was injected (1 mg; cat. no. SML1754; Sigma-Aldrich; Merck KGaA) into the anterior tibial muscle of the rats to establish a model of acute rat tibial anterior muscle injury. After 24 h of CTX injection, two rats were sacrificed and the successful model establishment was assessed by H&E staining and the rats were randomly divided into the following three groups (n=6 per group): Control; model; and EA. Rats in the control group was injected with 100 µl normal saline. In the EA group, the ‘Shenyu’ (the lower sides of the second lumbar vertebra) and ‘Housanli’ (posterolateral knee joint, ~5 mm below the fibular capitulum) acupoints were selected as sites for stimulation according to ‘Experimental Acupuncture’ and ‘Handbook of Acupuncture for Experimental Animals’. The rat's limbs were then fixed whilst the eyes of the rats were covered using a hood and the acupoints were punctured with a straight stainless-steel millineedle (0.22x15 mm). The EA therapeutic apparatus (Electronic acupuncture instrument SDZ II; Suzhou Medical Products Factory Co., Ltd.; https://www.hwato-med.com/product/detail.html?id=743) was then connected to the needles and the acupoints were stimulated at a frequency of 100-120 times/min at 2 mA under 100 Hz with a needle retention time of 20 min. The rats were stimulated once a day and intervention continued for 1 or 2 weeks. During this time, the rats were assessed for their mental, behavioral (mental: Excitement and movement; behavioral: Paralysis, flaccid disorder, spasticity, disorder and claudication), dietary and water intake. The rats in the model and control groups were not given additional stimulation. After 7 or 14 consecutive days of EA, nine rats were anesthetized with 3% sodium pentobarbital (40 mg/kg) before cervical dislocation under anesthesia. Rat tibialis anterior muscle tissues and blood samples were then collected and stored at -80˚C. All experimental procedures in the present study were performed in accordance with the requirements of the Ethics of Animal Experiments and approved by the Animal Care and Use Committee of Wuhan Myhalic Biotechnology Co. Ltd. (approval no. HLK-20181118-01).

H&E and Masson staining. Anterior tibial muscular tissues were fixed in 4% paraformaldehyde at 25˚C for 24 h and gradually rehydrated in a descending ethanol gradient. The tissues were then embedded in paraffin and sectioned at 3 µm per slice. The sections were baked in an oven at 60˚C for 40 min, followed by incubation in xylene for 10 min in an oven at 60˚C. The sections were then replaced with clean xylene and soaked again at 25˚C for 5 min, before being incubated in a decreasing ethanol gradient. For H&E staining, the sections were stained with hematoxylin for 5 min at room temperature and immersed in a 1% ethanolic hydrochloric acid solution for 30 sec to remove excess hematoxylin. Subsequently, the sections were counterstained with 5% eosin for 5 min at room temperature.

For Masson staining, the sections were stained with a mixture of hematoxylin staining solution and aqueous ferric chloride solution for 10 min, washed with a hydrochloric acid-ethanol fractionation solution in water for 15 sec and Masson bluing solution for 5 min, before being washed with distilled water for 1 min. They were then stained with Lichon red magenta staining solution for 5 min, washing with aqueous an acetic acid solution, aqueous phosphomolybdic acid solution and aqueous acetic acid solution in turn for 1 min each before staining with aniline blue. After staining for 2 min and washing again for 1 min, they were treated with anhydrous ethanol and xylene and mounted with neutral resin. All staining processes were performed at 25˚C. All prepared sections were observed under a light microscope at x200 magnification.

ELISA. Blood was collected and placed at 37˚C for 1-2 h, centrifuged at 1000 x g for 10 min at 4˚C and the supernatant was collected as serum. The levels IL-6, IL-4, IL-33, IL-10 and TNF-α in the serum were evaluated by ELISA. IL-6 (cat. no. RA20607), IL-4 (cat. no. RA20088), IL-33 (cat. no. RA21016), IL-10 (cat. no. RA20090), and TNF-α (cat. no. RA20035) ELISA kits were obtained from Bioswamp Life Science Lab; Wuhan Bein Lai Biotechnology Co., Ltd. The assay was performed according to the manufacturer's protocol and the optical density was measured at 450 nm using a microplate reader (Multiskan MS; Thermo Fisher Scientific, Inc.).

Immunofluorescence. The formalin-fixed paraffin-embedded tissue blocks were baked in an oven at 65˚C for 1 h to remove the wax blocks. The sections were placed in a descending ethanol gradient before being incubated in citric acid buffer at 125˚C and 103 KPa for 23 min, naturally cooled and rinsed three times with PBS. The sections were then blocked in 10% goat serum (cat. no. SL038; Beijing Solarbio Science & Technology Co., Ltd.) and incubated in a wet box at 25˚C for 10 min. The sections were then incubated overnight at 4˚C with CD86 (1:50; cat. no. PAB43783; Bioswamp Life Science Lab; Wuhan Bein Lai Biotechnology Co., Ltd.) and CD163 (1:50; cat. no. MA5-16656; Invitrogen; Thermo Fisher Scientific, Inc.) primary antibodies. Sections were then removed and rested at 25˚C for 40 min. After resting, the sections were incubated with Alexa Fluor 594-conjugated goat anti-rabbit IgG (1:20; cat. no. SA00006-4; Wuhan Sanying Biotechnology) and FITC-conjugated Affinipure Donkey Anti-Mouse IgG (1:20; cat. no. SA00003-9; Wuhan Sanying Biotechnology) secondary antibodies for 1 h at 37˚C. The slices were sealed at 25˚C using a Mounting Medium, antifading (with DAPI) (cat. no. S2110; Beijing Solarbio Science & Technology Co., Ltd.) and left for 30 min to stain the cell nuclei. Images were captured of 20 fields of view at x200 magnification with a fluorescence microscope (MD1000; Leica Microsystems GmbH). Quantification of the images was performed using Image J (v1.53e; National Institutes of Health)

Immunohistochemistry. The formalin-fixed, paraffin-embedded tissue blocks were placed at -20˚C for ≥30 min to increase hardness before slicing at a thickness of 4-µm. Before primary antibody incubation, the sections were heated and dewaxed using the procedure identical to that of H&E staining aforementioned. They were then rehydrated in a descending ethanol gradient and treated with 0.01 mmol/l sodium citrate buffer solution for 23 min at high pressure (125˚C and 103 kPa) for antigen retrieval. Elimination of endogenous peroxidase activity was performed by 3% hydrogen peroxide incubation at 25˚C for 10 min. The sections were then blocked with 10% goat serum (cat. no. SL038; Beijing Solarbio Science & Technology Co., Ltd.) for 30 min at 25˚C and incubated overnight at 4˚C with primary antibodies against Axin2 (1:50; cat. no. PAB40586; Bioswamp Life Science Lab; Wuhan Bein Lai Biotechnology Co., Ltd.), collagen type II (1:50; cat. no. PAB43834; Bioswamp Life Science Lab; Wuhan Bein Lai Biotechnology Co., Ltd.) and β-catenin (1:50; cat. no. PAB30671; Bioswamp Life Science Lab; Wuhan Bein Lai Biotechnology Co., Ltd.). Afterwards, the sections were incubated with a MaxVision™ HRP-Polymer anti-Mouse/Rabbit IHC Kit (cat. no. KIT-5020; Fuzhou Maixin Biotech Co., Ltd.; https://www.maxim.com.cn/sitecn/myzhjcxthsjh/1056.html) at 4˚C for 45 min, according to manufacturer's protocols. The sections were then stained using DAB (cat. no. DA1010-2 Beijing Solarbio Science & Technology Co., Ltd.). Finally, the sections were counterstained with Harris' hematoxylin at 25˚C for 3 min and evaluated by visual assessment of the staining intensity using a light microscope at x200 magnification with 20 of fields of view. Quantification of immunohistochemical images was performed using Image J (v1.53e; National Institutes of Health).

Western blotting. The relative protein expression levels were detected by western blotting. Protein was extracted by lysing muscle tissue cells using RIPA buffer (cat. no. PAB180006; Wuhan Bein Lai Biotechnology Co., Ltd.) and 20 µg of protein was quantified using the BCA protein concentration assay kit. The protein was resuspended in SDS sample buffer and boiled at 100˚C for 5 min. Equal amounts of total protein were then separated by 12% SDS-PAGE and then transferred onto PVDF membranes. The membranes were then incubated with 5% skimmed milk at 25˚C for 2 h before being incubated overnight at 4˚C with the following primary antibodies: TGF-β1 (1:2,000; cat. no. PAB33215; Wuhan Bein Lai Biotechnology Co., Ltd.), MMP-2 (1:2,000; cat. no. PAB30618; Wuhan Bein Lai Biotechnology Co., Ltd.), MMP-7 (1:2,000; cat. no. PAB30191; Wuhan Bein Lai Biotechnology Co., Ltd.), phosphorylated (p-) Smad3 (1:1,000; cat. no. ab193297; Abcam), Smad3 (1:2,000; cat. no. PAB30705; Wuhan Bein Lai Biotechnology Co., Ltd.), p-ERK1/2 (1:2,000; cat. no. PAB36335-P; Wuhan Bein Lai Biotechnology Co., Ltd.), ERK1/2 (1:2,000; cat. no. MAB37327; Wuhan Bein Lai Biotechnology Co., Ltd.), p-p38 (1:2,000; cat. no. PAB43139-P; Wuhan Bein Lai Biotechnology Co., Ltd.), p38 (1:2,000; cat. no. PAB38871; Wuhan Bein Lai Biotechnology Co., Ltd.) and GAPDH (1:2,000; cat. no. PAB36264; Wuhan Bein Lai Biotechnology Co., Ltd.). The membranes were next washed with TBS and incubated with HRP-conjugated goat anti-rabbit IgG secondary antibody (1:20,000, cat. no. PAB160011; Bioswamp Life Science Lab; Wuhan Bein Lai Biotechnology Co., Ltd.) for 2 h at 25˚C. Finally, the immunoreactivity was visualized by a colorimetric reaction using the enhanced chemiluminescence substrate buffer (EMD Millipore). The membranes were scanned using Gel Doz EZ imager (Bio-Rad Laboratories, Inc.). The gray value of the relevant bands was quantified using the TANON GIS software (version 4.2; Tanon Science and Technology Co., Ltd.).

Statistical analysis. Statistical analysis was performed with SPSS 19.0 software (IBM Corp.) using one-way analysis of variance followed by Tukey's test. Data are expressed as the mean ± standard deviation. $P<0.05$ was considered to indicate a statistically significant difference.

Results

General condition. After 7 days of adaptive feeding, a muscle injury model was constructed by injecting CTX. EA intervention was performed before the mental state, diet and activity of the rats were observed. None of the rats died during the experimental period. The weights of all rats remained stable without significant difference, and there was no significant difference among the treatment groups in terms of diet and water intake (data not shown). Compared with the control rats the mental state of the model rats gradually deteriorated, where their activity became limited. Compared with the model rats, the mental state and activity of the EA-treated rats were improved, which became more notable with intervention time (data not shown). Subsequently, 24 h after injection of CTX, HE staining revealed clear inflammatory cell infiltration in the tissues isolated from rats in the model group compare with those in the control group (Fig. 1). Since this cell type was

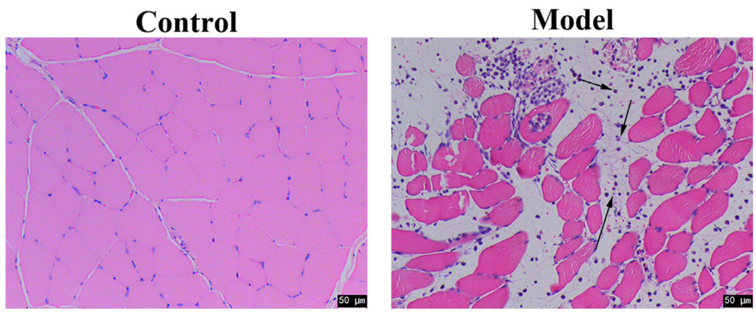

Figure 1. Muscle morphology and histology as observed by HE staining 24 h after cardiotoxin injection. Scale bars, 50 μm. n=2 rats.

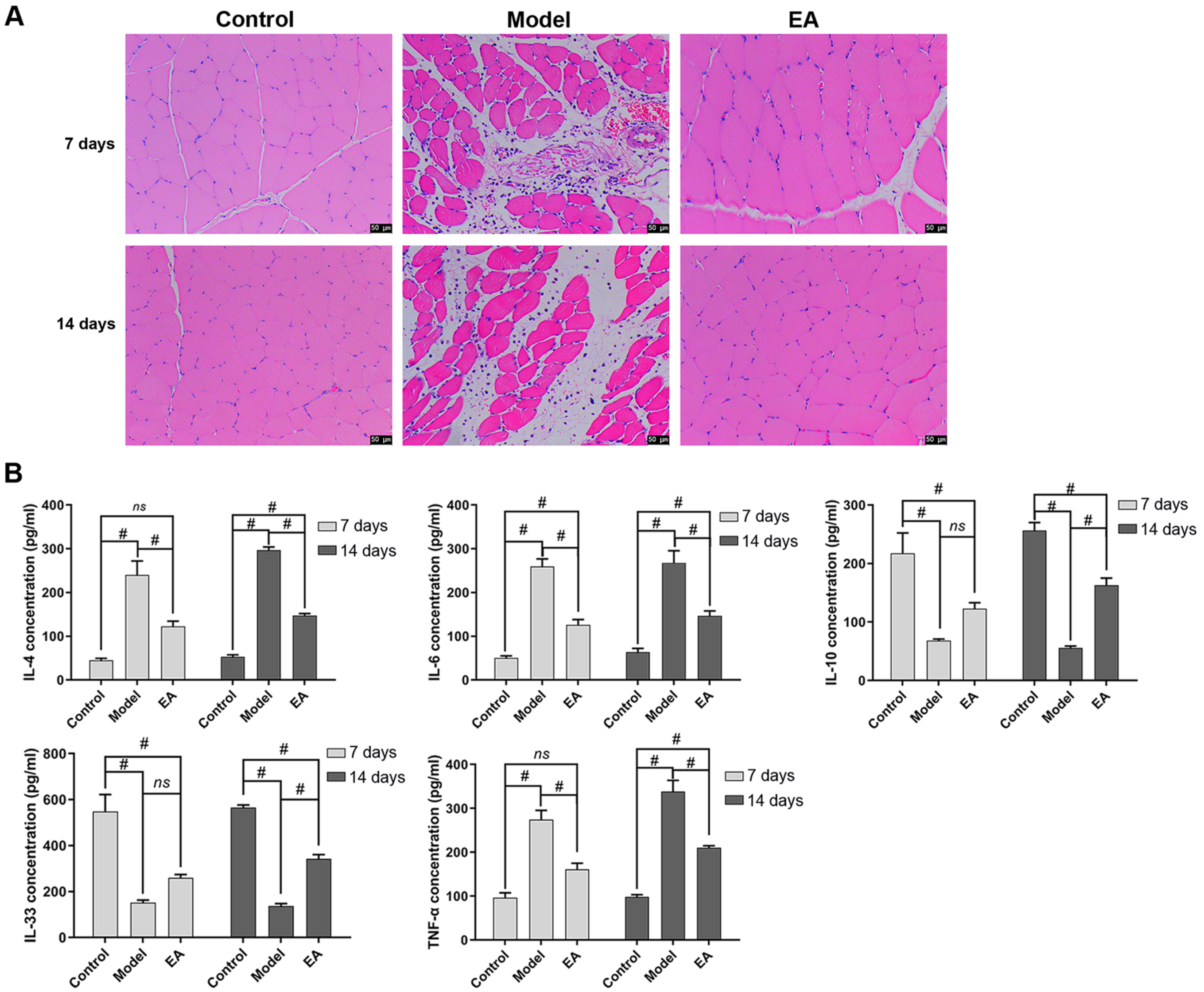

Figure 2. Effect of EA on inflammation in skeletal muscle fibrosis rat model. (A) Muscle morphology and histology in the three treatment groups was observed by H&E staining. (B) Serum levels of IL-6, IL-4, IL-33, IL-10 and TNF-α were measured by ELISA. $^{\#}$P<0.05. n=3 rats per group. EA, electroacupuncture; ns, not significant.

present, this suggests that this skeletal muscle injury model was successfully constructed.

EA alleviates skeletal muscle inflammation and fibrosis. To examine the effect of EA on the inflammatory response in rats with skeletal muscle injury, the degree of inflammatory infiltration in skeletal muscle tissues was assessed. Compared with that in the control group, the model group showed notable inflammatory infiltration (Fig. 2A). By contrast, after EA treatment, inflammatory infiltration was alleviated (Fig. 2A). Subsequently, changes in the levels of inflammation-related factors in the serum were measured (Fig. 2B). Compared

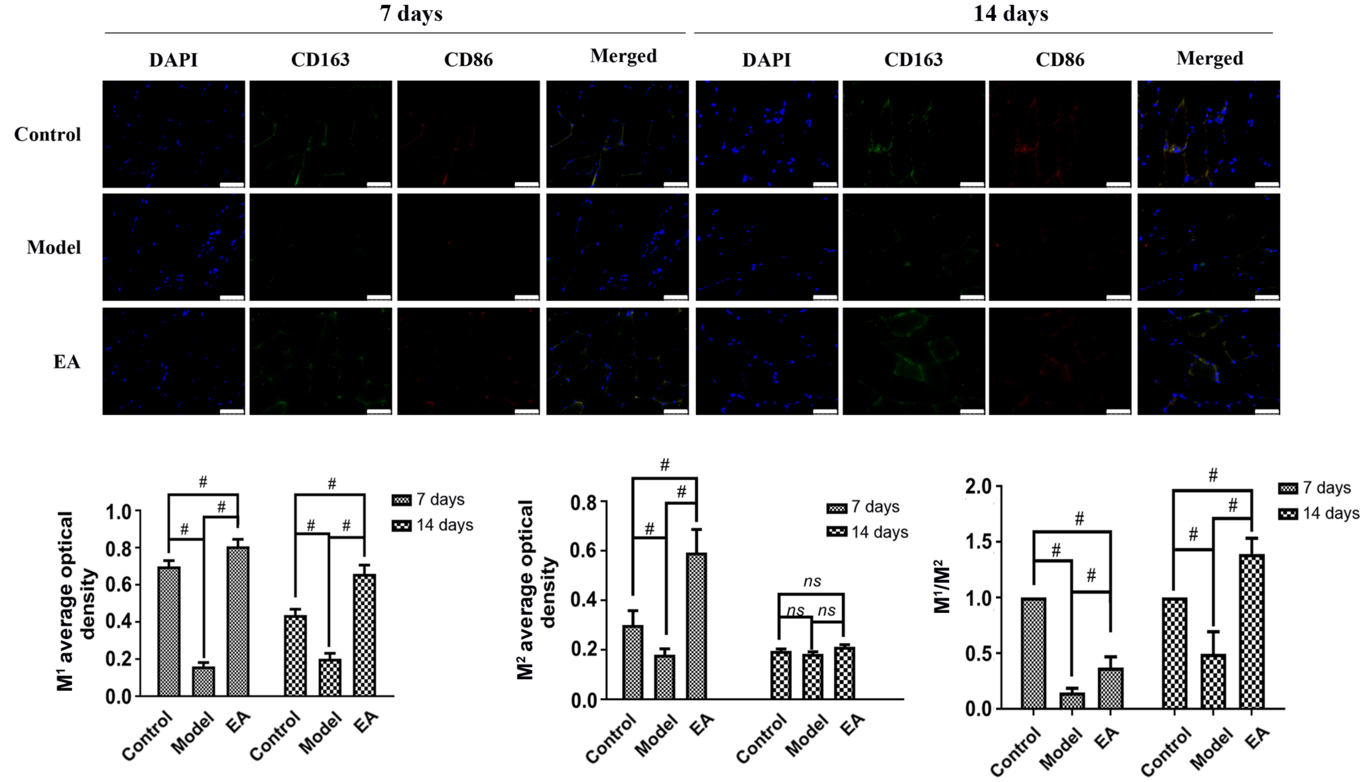

Figure 3. Effect of EA on the expression of M_1 and M_2 macrophage markers in muscle tissues. CD163 and CD86 expression were measured using immunofluorescence. Scale bars, 100 μm. n=3 rats per group. $^{\#}$P<0.05. EA, electroacupuncture; ns, not significant.

with those in the control group, the levels of IL-33 and IL-10 were significantly decreased in the model group, whilst that of IL-6, IL-4 and TNF-α was significantly increased on both days 7 and 14 (Fig. 2B). Compared with those in the model group, EA significantly increased the levels of of IL-33 and IL-10 on day 14 whilst significantly reducing those of IL-6, IL-4 and TNF-α on both days 7 and 14 (Fig. 2B).

EA promotes the transformation of macrophages from the M_1 into the M_2 sub-type. Immunofluorescence was next performed to detect the expression of surface markers of M_1 (CD86) and M_2 (CD163) macrophages in the muscle tissue (Fig. 3). On days 7 and 14, the average optical density of M_1 in the model group was significantly lower compared with that in the control group and EA groups (Fig. 3), whereas the trend of the mean optical density of M_2 at day 7 was similar to that of M_1 at day 7 (Fig. 3). In addition, the M_1/M_2 ratio was significantly increased by EA compared with model at both time points (Fig. 3).

EA suppresses collagen deposition and fibrosis in skeletal muscle. As shown in Fig. 4A, the model group showed greater levels of collagen II deposition in muscle tissues compared with that in the control and EA groups, suggesting that EA inhibited collagen deposition in muscle tissues. Immunohistochemistry was then performed to detect the expression of muscle fibrosis-related proteins Axin2, collagen II, β-catenin in muscle tissues (Fig. 4B). Compared with those in the control group, the expression levels of Axin 2, β-catenin and collagen II were significantly increased in the model group at both days 7 and 14 (Fig. 4B). However, compared with those in the model group, the expression levels of these muscle fibrosis-related proteins were significantly decreased after the EA intervention both at day 7 and day 14.

EA reduces skeletal muscle fibrosis through TGF-β1/Smad3/p38/ERK1/2 signaling. Western blotting was then performed to measure the protein expression of TGF-β1, MMP-2, MMP-7 and the activation of Smad3, p38 and ERK1/2 (Fig. 5). Compared with that in the control, the protein levels of TGF-β1, MMP-2, MMP-7 and p-p38 were significantly increased in the model at 7 and 14 days. By contrast, p-ERK1/2 levels were significantly higher in the model compared with those in the control at 7 days, whilst the opposite trend was observed at 14 days. The levels of p-Smad3 were decreased at both time points in the model compared with those in the control. The EA group had higher levels of p-ERK1/2 and p-Smad3 activation compared with those in the model group (Fig. 5), whilst the expression of TGF-β1, MMP-2, MMP-7 and p-p38 activation was significantly lower. These results remained consistent at day 7 and 14 (Fig. 5). This suggest that EA reduced skeletal muscle fibrosis through the TGF-β1/Smad3/p38/ ERK1/2 pathway.

Discussion

Acute skeletal muscle injury is common in sports and is typically caused by blunt trauma or stretch-induced injury (21). Previous studies have reported the ability of skeletal muscle fibers to regenerate and repair after acute skeletal muscle injury. However, muscle cell death would occur and the ability

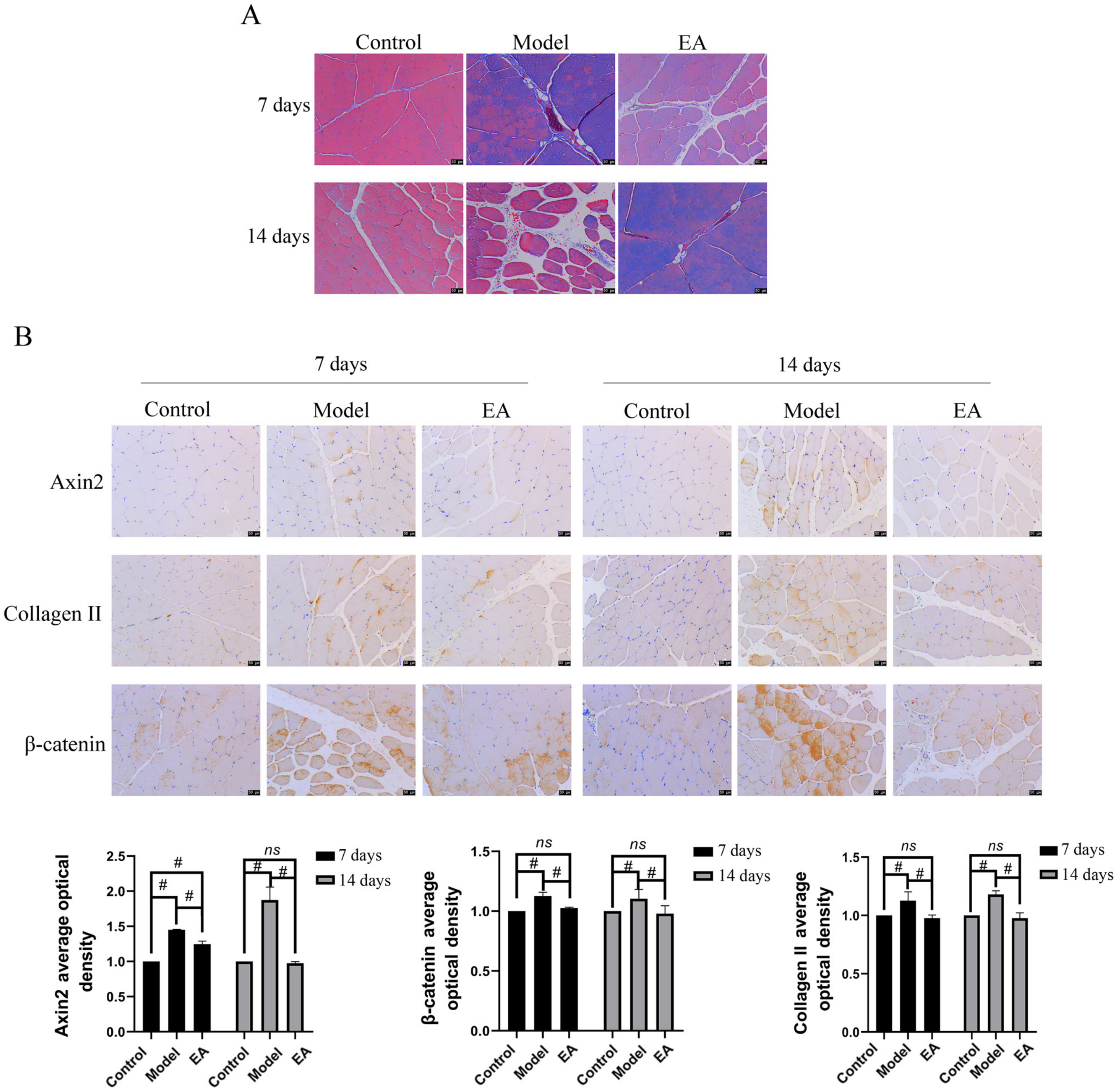

Figure 4. Effect of EA on skeletal muscle collagen deposition and fibrosis. (A) Collagen deposition was detected by Masson staining. (B) Expression of collagen II, Axin2 and β-catenin was measured by immunohistochemistry. Scale bars, 50 μm. n=3 rats per group. #P<0.05. EA, electroacupuncture.; ns, not significant.

to regenerate would be lost if a blunt trauma injury causes the skeletal muscle fibers to break, which can cause connective tissue proliferation, which in turn leads to bruise repair and skeletal muscle fibrosis (22,23). Due to the continuous infiltration by inflammatory cells, myoblasts can laterally differentiate into myofibroblasts, the excessive activation and proliferation of which can result in the production of a large quantities of extracellular matrix (24). This can lead to the continuous aggregation of collagen fibers, an important feature of skeletal muscle fibrosis (24). In the present study, it was revealed that EA significantly reduce collagen deposition in the skeletal muscle. Skeletal muscle fibrosis is generally irreversible and can lead to varying degrees of functional impairment and decreased exercise capacity (23). Therefore, targeting fibrosis has been a major research focus in the field of sports medicine.

As important cells in the innate immune system, macrophages exist in different subtypes based on the surrounding environment, which can in turn exert different roles (25). The most important subtypes are the M_1 and M_2 types (26). M1 macrophages are classically activated and mainly mediate immune functions (26). They can induce inflammatory damage by secreting proinflammatory mediators, including IL-6, monocyte chemoattractant protein-1 and TNF-α (25). By contrast, M_2 macrophages serve an anti-inflammatory role by secreting anti-inflammatory cytokines, such

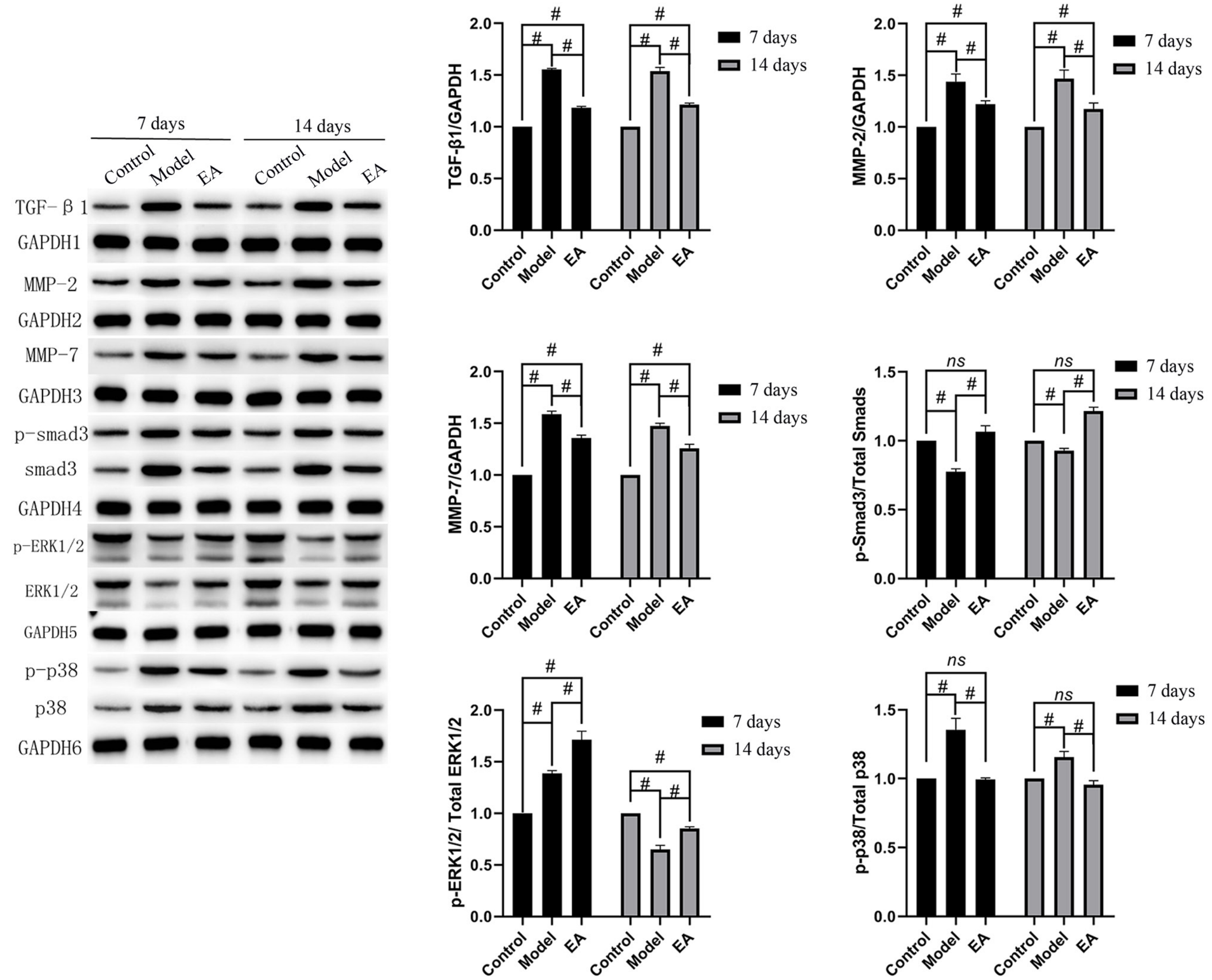

Figure 5. Effect of EA on the TGF-β1/Smad3/P38/ERK1/2 pathway in muscle tissues. Expression levels of TGF-β1, MMP-2, MMP7 and the phosphorylation levels of SMAD3, ERK1/2 and p38 were measured by western blotting. n=3 rats per group. #P<0.05. EA, electroacupuncture; ns, not significant.

as IL-10 (14). Acupuncture has been found to selectively regulate the phagocytic function of macrophages (27). Under normal physiological conditions, EA has little effect on the phagocytic function of macrophages (28). However, under pathological conditions, such as obesity, it can enhance phagocytosis, but when phagocytosis becomes excessive, the phagocytic index is reduced (28). Zhang *et al* (29) observed that in acupuncture-treated mice, the body mass was reduced, blood lipid levels and proinflammatory mediator release were decreased, whilst anti-inflammatory mediator release was promoted, iNOS expression was decreased and M_2 marker (CD206) expression was increased, compared with those in the model group. This suggests that acupuncture promoted the transformation of macrophages from M_1 to the M_2 subtype and reduced the inflammatory response in the epididymal white fat tissues (29). Data in the present study found that EA effectively upregulated expression of the M_1 and M_2 markers. In addition, the levels of IL-33 and IL-10 in the serum were increased by EA but the serum levels of IL-6, IL-4 and TNF-α were reduced.

MMPs are matrix-degrading enzymes that exert a variety of effects on the extracellular matrix. In total, 26 members of the MMP family have been identified to date, the majority of which share similar structures (30-33). The increased expression of MMPs assists in the formation of new muscle fibers at the injured site (33). According to its substrates, MMPs can be divided into the following four categories: Collagenase (MMP-1, -8, -13 and -18), gelatinase (MMP-2 and -9), interstitial lysin (MMP-3, -7, -10, -11 and -12), and membrane metalloproteinase (MMP-14, -15, -16 and -17) (34). A number of studies have shown that MMP-2 in skeletal muscle satellite cell migration and differentiation both in cultured muscle cells *in vitro* and in animal models *in vivo* (35,36), promoting tissue regeneration further (37). In addition, numerous studies have indicated that MMP-2 and MMP-7 serve an important role in myotube formation, such that they can regulate the degeneration and regeneration of muscle fibers in dystrophic muscle (37,38). Studies have also shown that MMP-2 participates in the migration of muscle-specific stem cells and myoblasts (39), where the elimination of MMP-2 from the skeletal muscle of Mdx-mice led to reduced angiogenesis and impaired muscle regeneration (40). Zheng *et al* (41) found that the expression of MMP-2 is related to CD206, suggesting that inhibiting the expression of MMP-2 can delay the progression of skeletal muscle fibrosis. In the present study, the expression of MMP-2 and TGF-β1 decreased significantly after EA. TGF-β1 inhibits myogenic cell proliferation *in vitro* and promotes the lateral differentiation of muscle cells into myofibroblasts (42). Macrophages M_1 can secrete TGF-β1, and the mRNA expression of which is increased after skeletal muscle injury (43). In the absence of macrophages, fewer new muscle fibers are formed, which then increases the fibrotic area (34). Therefore, macrophages may regulate the lateral differentiation of myoblasts by secreting TGF-β1, inhibiting the proliferation of muscle cells and participating in the occurrence and development of skeletal muscle fibrosis. EA may interfere with these processes and inhibit fibrosis.

TGF-β1 is the core regulatory factor in skeletal muscle fibrosis, such that the inhibition of TGF-β1 signaling has been shown to effectively inhibit skeletal muscle fibrosis (44). The upregulation of periostin can activate TGF-β signaling, where knocking out the periostin gene in mice with muscular dystrophy has been shown to significantly reduce skeletal muscle fibrosis (45). Bedair *et al* (46) used decorin to interfere with the function of TGF-β and observed that post-injury, regeneration of the skeletal muscle was promoted and the formation of fibrous tissues was reduced. Halofuginone is an antagonist of Smad3 phosphorylation that has been demonstrated to significantly suppress the expression of collagen and promote myogenesis in the skeletal muscle of mdx-mice whilst enhancing regeneration and functional recovery (47,48). In the present study, EA significantly reduced the activity of TGF-β1 and p38 and upregulated the expression of ERK1/2 and Smad3, suggesting that EA may exert therapeutic effects by regulating the activity of the TGF-β1/Smad3/p38/ERK1/2 signaling axis. However, there are some limitations in the present study, since no inhibitor of the TGF-β pathway was added, whether the regulation of this pathway by EA is influenced by other factors cannot be ruled out. Therefore, in further studies, this aspect should be considered to make the mechanistic role of EA in this signaling pathway clearer.

In conclusion, inhibit collagen deposition in skeletal muscle and alleviate inflammatory responses post-injury. The effect of EA may be achieved by regulating the TGF-β1/Smad3/p38/ERK1/2 signaling pathway.

Acknowledgements

Not applicable.

Funding

The present study is supported by the Wuhan Health and Family Planning Commission Research Project (grant no. WZ18D20).

Availability of data and materials

The datasets used and/or analyzed during the current study are available from the corresponding author on reasonable request.

Authors' contributions

HH and ML conceptualized and designed the study. HuL analyzed data. HaL performed the experiments. All authors have read and approved the final version of the manuscript. HH and ML confirm the authenticity of all the raw data.

Ethics approval and consent to participate

All experimental procedures in the present study were performed in accordance with the requirements of the Ethics of Animal Experiments and approved by the Animal Care and Use Committee of Wuhan Myhalic Biotechnology Co. Ltd. (approval no. HLK-20181118-01).

Patient consent for publication

Not applicable.

Competing interests

The authors declare that they have no competing interests.

References

1. Liao CH, Lin LP, Yu TY, Hsu CC, Pang JS and Tsai WC. Ibuprofen inhibited migration of skeletal muscle cells in association with downregulation of p130cas and CrkII expressions. Skelet Muscle 9: 23, 2019.
2. Huard J, Li Y and Fu FH: Muscle injuries and repair: Current trends in research. J Bone Joint Surg Am 84: 822-832, 2002.
3. Baoge L, Van Den Steen E, Rimbaut S, Philips N, Witvrouw E, Almqvist KF, Vanderstraeten G and Vanden Bossche LC: Treatment of skeletal muscle injury: A review. ISRN Orthop 2012: 689012, 2012.
4. Garg K, Corona BT and Walters TJ: Therapeutic strategies for preventing skeletal muscle fibrosis after injury. Front Pharmacol 6: 87, 2015.
5. McDermott MM, Dayanidhi S, Kosmac K, Saini S, Slysz J, Leeuwenburgh C, Hartnell L, Sufit R and Ferucci L. Walking Exercise Therapy Effects on Lower Extremity Skeletal Muscle in Peripheral Artery Disease. Circ Res 128: 1851-1867, 2021.
6. Mahdy MAA: Skeletal muscle fibrosis: An overview. Cell Tissue Res 375: 575-588, 2019.
7. Tsai WC, Yu TY, Chang GJ, Lin LP, Lin MS, Pang JS. Platelet-Rich Plasma Releasate Promotes Regeneration and Decreases Inflammation and Apoptosis of Injured Skeletal Muscle. Am J Sports Med Jul 46: 1980-1986, 2018.
8. Border WA and Noble NA: Transforming growth factor beta in tissue fibrosis. N Engl J Med 331: 1286-1292, 1994.
9. Delaney K, Kasprzycka P, Ciemerych MA and Zimowska M: The role of TGF-β1 during skeletal muscle regeneration. Cell Biol Int 41: 706-715, 2017.
10. Fang H, Judd RL. Adiponectin Regulation and Function. Compr Physiol 8: 1031-1063, 2018.
11. Delos D, Leineweber MJ, Chaudhury S, Alzoobaee S, Gao Y and Rodeo SA: The effect of platelet-rich plasma on muscle contusion healing in a rat model. Am J Sports Med 42: 2067-2074, 2014.
12. Li H, Hicks JJ, Wang L, Oyster N, Philippon MJ, Hurwitz S, Hogan MV and Huard J: Customized platelet-rich plasma with transforming growth factor β1 neutralization antibody to reduce fibrosis in skeletal muscle. Biomaterials 87: 147-156, 2016.
13. Wehling-Henricks M, Jordan MC, Gotoh T, Grody WW, Roos KP and Tidball JG: Arginine metabolism by macrophages promotes cardiac and muscle fibrosis in mdx muscular dystrophy. PLoS One 5: e10763, 2010.
14. Nozaki M, Ota S, Terada S, Li Y, Uehara K, Gharaibeh B, Fu FH and Huard J: Timing of the administration of suramin treatment after muscle injury. Muscle Nerve 46: 70-79, 2012.
15. Ifrim Chen F, Antochi AD, Barbilian AG. Acupuncture and the retrospect of its modern research. Rom J Morphol Embryol 60: 411-418, 2019.

16. Martins L, Gallo CC, Honda TSB, Alves PT, Stilhano RS, Rosa DS, Koh TJ and Han SW: Skeletal muscle healing by M1-like macrophages produced by transient expression of exogenous GM-CSF. Stem Cell Res Ther 11: 473, 2020.
17. Li JP, Xu T and Xu SS: Expression and significance of TNF-α and MMP-1 in acupuncture to inhibit skeletal muscle fibrosis. Annual Meeting of Sports Physiology Committee of Chinese Physiological Society and Academic Seminar on 'Sports and Health', 2013.
18. Chen JDZ, Ni M, Yin J. Electroacupuncture treatments for gut motility disorders. Neurogastroenterol Motil 30: e13393, 2018
19. Han H and Li M: Clinical observation of acupuncture combined with exercise therapy for acute lumbar sprain. Lishizhen Med Mater Med Res 23: 244-245, 2012.
20. Zhang J, Xiao Z, Qu C, Cui W, Wang X and Du J: CD8 T cells are involved in skeletal muscle regeneration through facilitating MCP-1 secretion and Gr1(high) macrophage infiltration. J Immunol 193: 5149-5160, 2014.
21. Bayer ML, Magnusson SP, Kjaer M, Tendon Research Group Bispebjerg. Early versus Delayed Rehabilitation after Acute Muscle Injury. N Engl J Med 377: 1300-1301, 2017.
22. Tidball JG: Mechanisms of muscle injury, repair, and regeneration. Compr Physiol 1: 2029-2062, 2011.
23. Smith RS and Chang FC: Traumatic rupture of the aorta: Still a lethal injury. Am J Surg 152: 660-663, 1986.
24. Deng XY, Wu ZB and Yang Z: Fibrosis in skeletal muscle:celluar and molecular mechanism. Chin J RHP 20: 142-147, 2014.
25. DeNardo DG, Ruffell B. Macrophages as regulators of tumour immunity and immunotherapy. Nat Rev Immunol Jun 19: 369-382, 2019.
26. Xia Y, Rao L, Yao H, Wang Z, Ning P and Chen X: Engineering Macrophages for Cancer Immunotherapy and Drug Delivery. Adv Mater 32: e2002054, 2020.
27. Zhang J, Xiao Z, Qu C, Cui W, Wang X, Du J. CD8 T cells are involved in skeletal muscle regeneration through facilitating MCP-1 secretion and Gr1(high) macrophage infiltration. J Immunol 193: 5149-5160, 2014.
28. Zhou SN, Xu YY and Hu HT: Research progress of acupuncture therapy on immune cells. Zhejiang JTradit Chin Med 55: 74-75, 2020.
29. Zhang SY, Hu X and Tang H: Effect of acupuncture on white adipose tissue macrophage polarization induced by high fat diet in obese mice. Chin Acupunc 37: 1205-1211, 2017.
30. Ding J, Chang YY, Li WJ, Guo B, Lu M and Collage XM: The effects of DAPT intervention on the expression of α-SMA and MMP-1/TIMP-1 in rats cardiac fibroblasts. J Clin Cardiol 32: 735-738, 2016.
31. Wang SQ, Chang Y, Ma XW and Wang F: Effects of endurence exercise of different intensity on cardiac collagen of rats and regulation of MMP-1/TIMP-1. Chi Sport Sci Technol 51: 60-66, 2015.
32. Wang QY, Wang WJ, Xi J, Cai K, Wang P, Liang JD, Han J and He GZ: Effect of polysaccharides from eucommiae cortex on expressions of genes of I, III collagen, MMP-1, TIM MP-1 and TGF-β1 from hepatic fibrosis in rat models. Chin J Exp Trad Med Formu 24: 153-158, 2018.
33. Spinale FG: Myocardial matrix remodeling and the matrix metalloproteinases: Influence on cardiac form and function. Physiol Rev 87: 1285-1342, 2007.
34. Xiao W, Liu Y and Chen P: Macrophage depletion impairs skeletal muscle regeneration: The roles of pro-fibrotic factors, inflammation, and oxidative stress. Inflammation 39: 2016-2028, 2016.
35. Gihring A, Gärtner F, Liu C, Hoenicka M, Wabitsch M, Knippschild U, Xu P. Influence of Obesity on the Organization of the Extracellular Matrix and Satellite Cell Functions After Combined Muscle and Thorax Trauma in C57BL/6J Mice. Front Physiol 11: 849, 2020.
36. Dong G, Wang M, Gu G, Li S, Sun X, Li Z, Cai H and Zhu Z: MACC1 and HGF are associated with survival in patients with gastric cancer. Oncol Lett 15: 3207-3213, 2018.
37. Nalbandian M, Radak Z, Takeda M. Lactate Metabolism and Satellite Cell Fate. Front Physiol 11: 610983, 2020.
38. Chen X and Li Y: Role of matrix metalloproteinases in skeletal muscle: Migration, differentiation, regeneration and fibrosis. Cell Adhes Migr 3: 337-341, 2009.
39. Zheng LF, Chen LF, Chen PJ and Xiao WH: Fat deposition in skeletal muscle and its regulatory mechanism. Acta Physiologica Sinicaa 69: 344-350, 2017 (in Chinese).
40. Miyazaki D, Nakamura A, Fukushima K, Yoshida K, Takeda S and Ikeda S: Matrix metalloproteinase-2 ablation in dystrophin-deficient mdx muscles reduces angiogenesis resulting in impaired growth of regenerated muscle fibers. Hum Mol Genet 20: 1787-1799, 2011.
41. Zheng LF: Study on the role and mechanism of macrophages in the repair of skeletal muscle contusion. Shanghai university of sport, 2018 (in Chinese).
42. Carlson ME, Conboy MJ, Hsu M, Barchas L, Jeong J, Agrawal A, Mikels AJ, Agrawal S, Schaffer DV and Conboy IM: Relative roles of TGF-beta1 and Wnt in the systemic regulation and aging of satellite cell responses. Aging Cell 8: 676-689, 2009.
43. Fjeldborg K, Pedersen SB, Møller HJ, Christiansen T, Bennetzen M and Richelsen B: Human adipose tissue macrophages are enhanced but changed to an anti-inflammatory profile in obesity. J Immunol Res 2014: 309548, 2014.
44. Rana T, Jiang C, Liu G, Miyata T, Antony V, Thannickal VJ and Liu RM: PAI-1 Regulation of TGF-β1-induced Alveolar Type II Cell Senescence, SASP Secretion, and SASP-mediated Activation of Alveolar Macrophages. Am J Respir Cell Mol Biol 62: 319-330, 2020.
45. Lorts A, Schwanekamp JA, Baudino TA, McNally EM and Molkentin JD: Deletion of periostin reduces muscular dystrophy and fibrosis in mice by modulating the transforming growth factor-β pathway. Proc Natl Acad Sci USA 109: 10978-10983, 2012.
46. Bedair HS, Karthikeyan T, Quintero A, Li Y and Huard J: Angiotensin II receptor blockade administered after injury improves muscle regeneration and decreases fibrosis in normal skeletal muscle. Am J Sports Med 36: 1548-1554, 2008.
47. Roffe S, Hagai Y, Pines M and Halevy O: Halofuginone inhibits Smad3 phosphorylation via the PI3K/Akt and MAPK/ERK pathways in muscle cells: Effect on myotube fusion. Exp Cell Res 316: 1061-1069, 2010.
48. Huebner KD, Jassal DS, Halevy O, Pines M and Anderson JE: Functional resolution of fibrosis in mdx mouse dystrophic heart and skeletal muscle by halofuginone. Am J Physiol Heart Circ Physiol 294: H1550-H1561, 2008.